



HAL
open science

(P,N,P)Pd-versus (P,N,P)Ni-Catalyzed Suzuki-Miyaura Cross-Coupling Reactions under Green Conditions

Vincent Fagué, Diogo dos Santos, Jean-claude Daran, Sonia Mallet-ladeira, Pascal Guillo, Christophe Fliedel

► **To cite this version:**

Vincent Fagué, Diogo dos Santos, Jean-claude Daran, Sonia Mallet-ladeira, Pascal Guillo, et al.. (P,N,P)Pd-versus (P,N,P)Ni-Catalyzed Suzuki-Miyaura Cross-Coupling Reactions under Green Conditions. *European Journal of Inorganic Chemistry*, In press, 10.1002/ejic.202400729 . hal-04939963

HAL Id: hal-04939963

<https://hal.science/hal-04939963v1>

Submitted on 11 Feb 2025

HAL is a multi-disciplinary open access archive for the deposit and dissemination of scientific research documents, whether they are published or not. The documents may come from teaching and research institutions in France or abroad, or from public or private research centers.

L'archive ouverte pluridisciplinaire **HAL**, est destinée au dépôt et à la diffusion de documents scientifiques de niveau recherche, publiés ou non, émanant des établissements d'enseignement et de recherche français ou étrangers, des laboratoires publics ou privés.



Distributed under a Creative Commons Attribution - NonCommercial - NoDerivatives 4.0 International License

bis(diphenylphosphino)amine-type ligands, formally resulting from the functionalization of the N atom from DPPA by a substituent (alkyl or aryl) incorporating a chemical function/heteroatom (Figure 1).^[16] While the *P,P*-donor set remains untouched, and still provides a platform for the construction of mono-, di-, tri- or polynuclear complexes, the presence of an additional donor or reactive function on the *N*-tail allows i) to expand the denticity of the ligand and therefore the formation of coordination polymers or compounds of higher nuclearity,^[18–22] ii) the grafting on solid support,^[23] and iii) hypothetically the stabilization of reactive catalytic intermediates.^[24] While the choice of the function/heteroatom is sometimes obvious depending on the target reactivity, *e.g.* a thiol or thioether for Au surface functionalization, the nature of the linker (between the N atom and the additional function) has to be considered and is sometimes non-innocent.^[20–21] Another interesting feature of such ligands is the easy access to their mono-oxide, sulfide and selenide derivatives, leading to hybrid *P,P=X* (*X*=O, S, Se) ligands with an increased bite-angle forming five-membered metallacycles *vs.* four-membered metallacycles for the *P,P* versions.^[25] Such modification, *i.e.* from *P,P* to *P,P=X*-type ligand, strongly affects the stability, the reactivity and the catalytic performances of the resulting metal complexes.^[24,26–27]

Catalytic applications of metal complexes of *N*-functionalized DPPA-type ligands remain mainly focused on Ni- and Cr-catalyzed ethylene oligomerization/polymerization, Ru- and Rh-catalyzed transfer hydrogenation of ketones and Pd-catalyzed cross-coupling reactions.^[16–17,28] The importance of these reactions is no more to be discussed.^[29–34] However, due to environmental (availability, toxicity, waste) and economic issues, these reactions are still thoroughly studied, with the aim to

improve the catalytic systems (lower catalyst loading, lower reaction temperature and time, greener solvents etc).^{see e.g.[35–38]} In this regard, many research groups are working hard to substitute palladium by nickel catalysts in several reactions, such as cross-coupling reactions.^[39–42]

In the present contribution, in a first time, we evaluated a series of palladium(II) complexes of *N*-substituted/functionalized DPPA-type ligands, with various *N*-substituents, in Suzuki-Miyaura cross-coupling reactions, under so-called standard reaction conditions, to determine if the nature of the *N*-substituent affects the catalysts performances. In a second time, analog nickel(II) complexes were applied to this benchmark reaction, under “greener” conditions, to determine if these more sustainable catalytic systems can challenge “historical” catalysts.

Results and Discussion

Synthesis, Characterization and Solid-State Structures

DPPA-Type Ligands

In order to evaluate the influence of the *N*-substituent of DPPA-type ligands in Suzuki-Miyaura cross-coupling reactions, a series of five ligands were selected (1-5, Table 1 – Entry 1). This series consists of one ligand with an *N*-alkyl chain (1), one with an unfunctionalized *N*-aryl group (2), two ligands with different *para*-functions on the *N*-aryl group (3 (OMe) and 4 (SMe)), and one ligand with the functionalization in another position (*meta*-SMe for 5 *vs.* *para*-SMe for 4). While most of these ligands were already reported and synthesized according to reported

Table 1. ³¹P{¹H} NMR chemical shifts (in ppm) of ligands 1-5, palladium(II) complexes 6-10 and nickel(II) complexes 11-15 in CDCl₃ (a) or CD₂Cl₂ (b) at 25 °C. (c) A value of 70.1 ppm (in CDCl₃), which is clearly out of the range of all other published complexes of that type, was reported in Ref. [54].

	1	2	3	4	5
Free ligand					
δ (ppm)	63.49 ^(a)	69.8 ^(a)	70.0 ^(a)	69.4 ^(a)	69.02 ^(b)
Ref.	[55]	[56]	[52]	[57]	This work
Se ₂	1·Se ₂	2·Se ₂	3·Se ₂	4·Se ₂	5·Se ₂
δ (ppm)	68.33 ^(a)	69.69 ^(a)	70.13 ^(a)	70.06 ^(a)	69.71 ^(a)
¹ J _{P-Se} (Hz)	783	794	792	794	796
PdCl ₂	6	7	8	9	10
δ (ppm)	31.01 ^(b)	34.1 ^(b)	35.77 ^{(b),(c)}	35.27 ^(b)	34.43 ^(b)
Ref.	This work	[58]	This work and ^[54]	This work	This work
NiCl ₂	11	12	13	14	15
δ (ppm)	42.9 ^(b)	45.09 ^(a)	47.6 ^(a)	45.4 ^(b)	44.88 ^(b)
Ref.	[26]	This work	[52]	[24]	This work

procedures (see Table 1 and Experimental section), the *N,N*-bis(diphenylphosphino)-3-(methylthio)aniline ligand **5** was until now not described. Its preparation was readily achieved by reaction between the corresponding 3-(methylthio)aniline and 2 equivalents of PPh_2Cl in the presence of excess NEt_3 as HCl scavenger. Ligand **5** was isolated as an off-white powder in 78% yield, >90% purity (based on NMR analysis), characterized by multinuclear NMR and FT-IR spectroscopic techniques and mass spectrometry (ESI-MS), and was used for the complexation reactions without further purification (Scheme 1). Ligand **5** exhibits a typical singlet resonance at $\delta = 69.02$ ppm in its $^{31}\text{P}\{^1\text{H}\}$ NMR spectrum (Figure S1a in the ESI), which is found in the same range than the other *N*-aryl DPPA-type ligands **2–4** and downfield shifted compared to the *N*-alkyl DPPA-type ligand **1** (see Table 1). As explained above, ligand **5** was not obtained in a pure form and the different attempts to purify it were unsuccessful. The impurities, detected by $^{31}\text{P}\{^1\text{H}\}$ NMR as several peaks of very small intensity (Figure S1a in the ESI), may result from the degradation of a small part of the ClPPh_2 reagent during the course of the reaction. Therefore, it was used for complexation as obtained, the impurities did not appear to interfere in the complexation process, and could be easily removed from final complexes afterwards, leading to pure Pd^{II} and Ni^{II} complexes (see Experimental section and ESI).

To assay and compare the donor strength of the diphosphine ligands (**1–5**) used in this study, which may further help to rationalize their catalytic performances (together with steric factors, see following sections), we analyzed the P–Se coupling constants ($J_{\text{P–Se}}$) of their, *in-situ* generated, diselenated derivatives ($1\text{-Se}_2\text{-5-Se}_2$, see Experimental section and ESI). Indeed, several studies have shown that the magnitude of the $^1J_{\text{P–}^{77}\text{Se}}$ ($^{31}\text{P}\text{-}^{77}\text{Se}$) is strongly dependent upon the nature of the organic groups bound to the P atom, $^{[43-44]}$ which influences the *s* character of the P–Se bond through hybridization changes as predicted by Bent's rule. $^{[45]}$ While EWGs increase the *s* character of the P–Se bond, and thereby the $J_{\text{P–Se}}$ coupling constant, EDGs have the opposite effect. $^{[43-44]}$ It has recently been shown that a good correlation exists between the Tolman electronic parameter (TEP) of selected phosphines and the $J_{\text{P–Se}}$ of their respective phosphine selenides, $^{[46]}$ therefore the latter method represents a convenient alternative to the former to measure the donor ability of phosphine ligands. Oxidation of ligands **1–5** to their diselenated counterparts $1\text{-Se}_2\text{-5-Se}_2$ was readily achieved by room temperature reaction between the former and excess grey selenium in CDCl_3 . While only a negligible shift of the ^{31}P resonances, between 0.1 and 0.7 ppm, was observed when going from **2–5** to $2\text{-Se}_2\text{-5-Se}_2$, a much larger difference, *ca.*

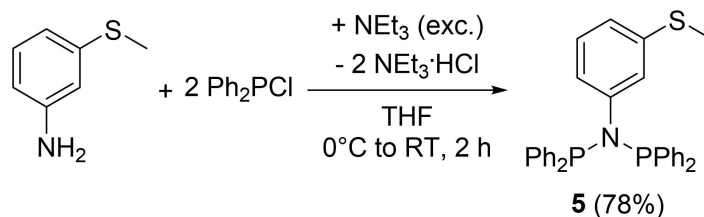
5 ppm, was observed for the $1/1\text{-Se}_2$ couple (Table 1). Similarly, the $^1J_{\text{P–Se}}$ measured for 1-Se_2 (783 Hz) is significantly smaller than those measured for the other diselenated species $2\text{-Se}_2\text{-5-Se}_2$ (792–796 Hz, Table 1), which may indicate a slightly stronger donor ability of **1** vs. **2–5**. Both the chemical shifts and the $^1J_{\text{P–Se}}$ values mentioned above were found in the same ranges than those reported for related diselenated bis(diphenylphosphino)amine-type ligands. $^{[47-49]}$ Steric factors are discussed on the basis of the steric maps of the available structures of the Pd and Ni complexes in the following sections.

Palladium(II) Complexes of DPPA-Type Ligands

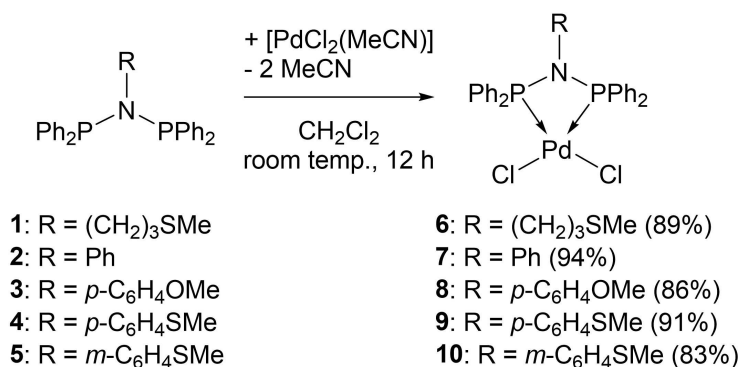
The procedure to access group 10 metal complexes of the type $[\text{MX}_2(\text{P},\text{P})]$ (with $\text{M} = \text{Ni}, \text{Pd}, \text{Pt}$; $\text{P},\text{P} = \text{DPPA-type ligand}$ and $\text{X} = \text{Cl}, \text{Br}$) is well-established and consists in the reaction of the desired DPPA-type ligand with a $[\text{MX}_2\text{L}_2]$ ($\text{L}_2 = \text{labile ligand(s)}$, such as COD, DME, 2 PhCN, 2 MeCN) or MX_2 precursor. Indeed, the equimolar reaction between the DPPA-type ligands (**1–5**) and either $[\text{PdCl}_2(\text{COD})]$ (COD = cycloocta-1,5-diene) or $[\text{PdCl}_2(\text{MeCN})_2]$ in dichloromethane at room temperature afforded the corresponding palladium(II) complexes (**6–10**, respectively) in high yields as pale yellow powders (Scheme 2). All the complexes were characterized by multinuclear NMR and FT-IR spectroscopic methods, ESI-MS and elemental analysis (EA). The synthesis of complexes **7** and **8** was already reported, however we provide here complementary analytical data (see Experimental section).

The $^{31}\text{P}\{^1\text{H}\}$ NMR spectra of the palladium(II) complexes **6–10** exhibited all one singlet resonance, for the two equivalent P atoms, between 31.01 and 35.77 ppm, upfield shifted of *ca.* 30–35 ppm with respect to the free ligands (Table 1). As for the free ligands, the compound that resonates at the lower frequency is the *N*-alkyl derivative (**6**). The recorded values are in agreement with the literature, since $^{31}\text{P}\{^1\text{H}\}$ NMR signals for PdCl_2 complexes of *N*-alkyl- and *N*-aryl-functionalized DPPA-type ligands were observed in the 30–36 and 34–42 ppm ranges, respectively. $^{[16]}$

X-ray diffraction (XRD) studies on yellow crystals obtained by slow diffusion of pentane into a saturated dichloromethane solution of **6** and chloroform solution of **8** revealed the structures depicted in Figure 2. As expected, the palladium(II) centers adopt a distorted square-planar geometry with diphosphines **1** and **3** acting as chelates and thus forming four-membered metallacycles, and the coordination spheres are completed by two chloride ligands. The slight distortion of the



Scheme 1. Synthesis of ligand **5**.



Scheme 2. Synthesis of the palladium(II) dichloride complexes 6-10.

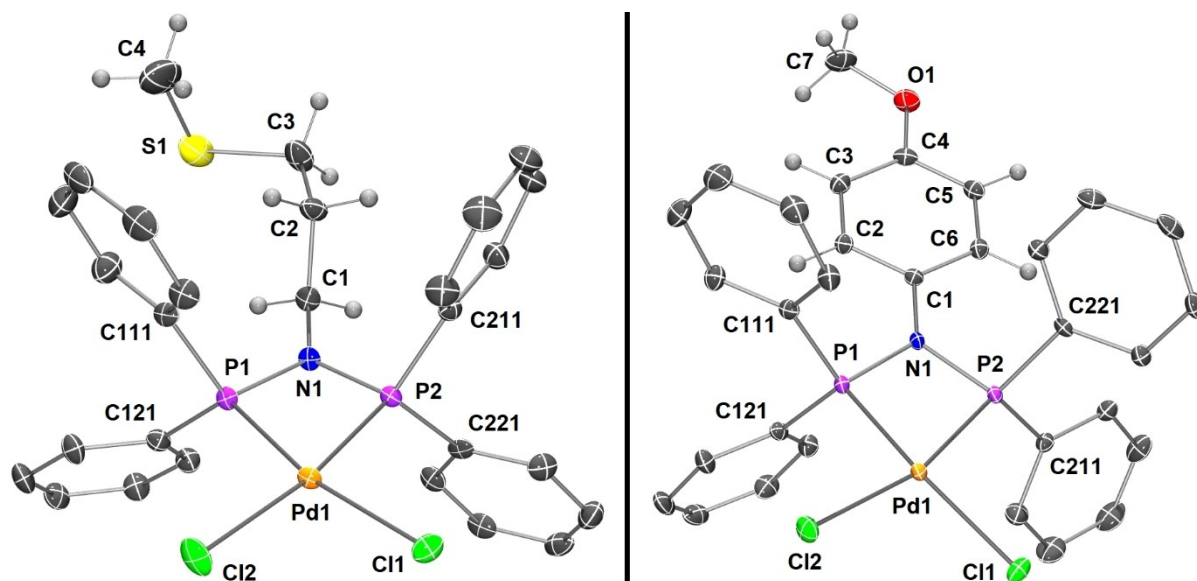


Figure 2. View of the molecular structures of complexes 6 (left) and 8 in 8·2CHCl₃ (right). Ellipsoids are represented at the 50% probability level. H atoms of the P-Ph rings are omitted for clarity. Selected bond distances (Å) and angles (deg) are listed in Table 2. ORTEP views of the asymmetric units of the crystal structures with labeling of all non-H atoms, crystal data and structure refinement parameters are available in the ESI.

coordination geometry from ideal square-planar is reflected by the calculated $\tau_4^{[50]}$ (0.17 for **6** and 0.18 for **8**) and $\tau_4^{[51]}$ (0.16 for **6** and 0.17 for **8**) parameters for each structure (see ESI for more details). Unless the P1-Pd1 (2.1663(5) Å) bond length in **8**·2CHCl₃, which is unusually short probably due to the involvement of Cl1 (*trans* to P1) in two H-bonds with two CHCl₃ molecules (see ESI - Figure S10), the other characteristic P-Pd, Pd-Cl and P-N bond lengths (Table 2) were found in the same ranges than the other PdCl₂ complexes of *N*-functionalized DPPA-type ligands.^[16]

Nickel(II) Complexes of DPPA-Type Ligands

The reaction between the DPPA-type ligands 1-5 and [NiCl₂(DME)] (DME = 1,2-dimethoxyethane) in a 1:1 ratio led to brick red powders of the corresponding nickel(II) complexes 11-15, respectively, in good yields (see Scheme 3 and ESI). Complexes 11 and 14 were already reported by us,^[24,26] complex

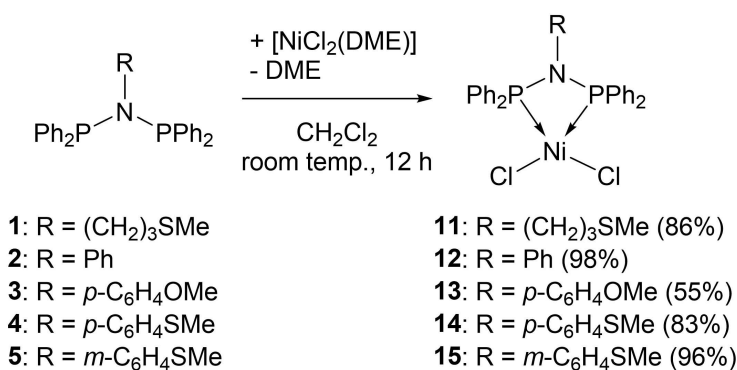
13 by Zhu, Lin and co-workers^[52] and complex **12** by Seidel and Alexiev (from NiCl₂·6H₂O).^[53] The latter was characterized by UV-Vis, FT-IR and EA, therefore we provide here additional characterization data, namely multinuclear NMR and XRD. Complex **15** is new and was thoroughly characterized, by multinuclear NMR and FT-IR spectroscopic methods, ESI-MS, EA and XRD (see Experimental section and ESI). Indeed, the diamagnetic character of complexes **12** and **15** allowed their characterization by multinuclear NMR, and in both cases the two equivalent phosphorous atoms of the coordinated ligand gave rise, as expected, to a singlet in ³¹P{¹H} NMR at 45.09 and 44.88 ppm, respectively, in the typical range for such complexes (Table 1).^[16] In the ¹H NMR spectra of complexes **12** and **15**, all the protons of the *N*-substituent could be attributed, while the *P-Ph* protons gave rise to three multiplets at δ = 8.04, 7.71, 7.57 ppm, counting for 8H, 4H and 8H, respectively. The *N-Ph* and *N*-(3-SMe)C₆H₄ protons of **12** and **15**, respectively, resonate at lower chemical shifts (vs. *P-Ph*) and give rise, as expected, to three (δ = 7.03 (1H), 7.01 (2H), 6.51 (2H) ppm) and four (δ = 6.91

Table 2. Selected bond lengths (Å) and angles (deg) in the solid-state structures of **6**, **8**-2CHCl₃, **12** and **15**. (M1 = Pd in **6** and **8**-2CHCl₃, M1 = Ni in **12** and **15**)

	6	8 -2CHCl ₃	12	15
M1-P1	2.2257(14)	2.1663(5)	2.1173(8)	2.1157(5)
M1-P2	2.2120(14)	2.2026(5)	2.1096(7)	2.1175(5)
M1-Cl1	2.3579(14)	2.3410(5)	2.1922(8)	2.1839(5)
M1-Cl2	2.3461(15)	2.3289(5)	2.1903(8)	2.2010(5)
P1-N1	1.697(5)	1.6911(15)	1.708(2)	1.7070(14)
P2-N1	1.695(5)	1.6949(15)	1.706(2)	1.7083(14)
N1-C1	1.476(7)	1.424(2)	1.442(6)	1.426(2)
P1-M1-P2	71.91(5)	72.133(17)	74.29(3)	74.486(18)
Cl1-M1-Cl2	95.36(5)	96.041(17)	99.77(4)	100.359(19)
P1-M1-Cl2	97.25(5)	92.845(17)	165.89(3)	169.31(2)
P2-M1-Cl1	95.49(5)	99.291(17)	168.58(4)	163.99(2)
P1-M1-Cl1	167.36(5)	168.959(17)	94.30(3)	90.020(18)
P2-M1-Cl2	169.15(5)	164.575(17)	91.64(3)	95.321(18)
P1-N1-P2	100.4(2)	98.87(8)	96.74(11)	97.20(7)

(1H), 6.90 (1H), 6.31 (1H), 6.18 (1H) ppm signals, respectively. The chemical shift corresponding to the SCH₃ moiety in **15** (δ = 1.93 ppm) is very close to this of the free ligand **5** (δ = 1.97 ppm), indicating that no coordination of the thioether function occurs in solution. A similar observation was made for complexes **11** and **14** that also bear a thioether function.^[24,26]

The solid-state structures of complexes **11**, **13** and **14** were already reported, by us (**11** and **14**)^[24,26] or Zhu and Lin and coworkers. (**13**).^[52] The molecular structures of complexes **12** and **15** were determined by single crystal X-ray crystallographic studies and confirmed, as expected and as in the aforementioned complexes, the presence of tetra-coordinated nickel centers in a distorted square-planar environment, with the diphosphine ligands, **2** and **5**, respectively, acting as chelates and forming four-membered metallacycles (Figure 3). The coordination spheres of the metal centers are completed by two chlorine atoms. The slight distortion of the coordination geometry from ideal square-planar is reflected by the calculated τ_4 ^[50] (0.18 for **12** and 0.19 for **15**) and τ_4' ^[51] (0.17 for **12** and 0.17 for **15**) parameters for both structures (see ESI for more details). The τ_4 and τ_4' parameters were also calculated for the other nickel(II) complexes studied in the present manuscript, *i.e.* **11**,



Scheme 3. Synthesis of the nickel(II) dichloride complexes **11**-**15**.

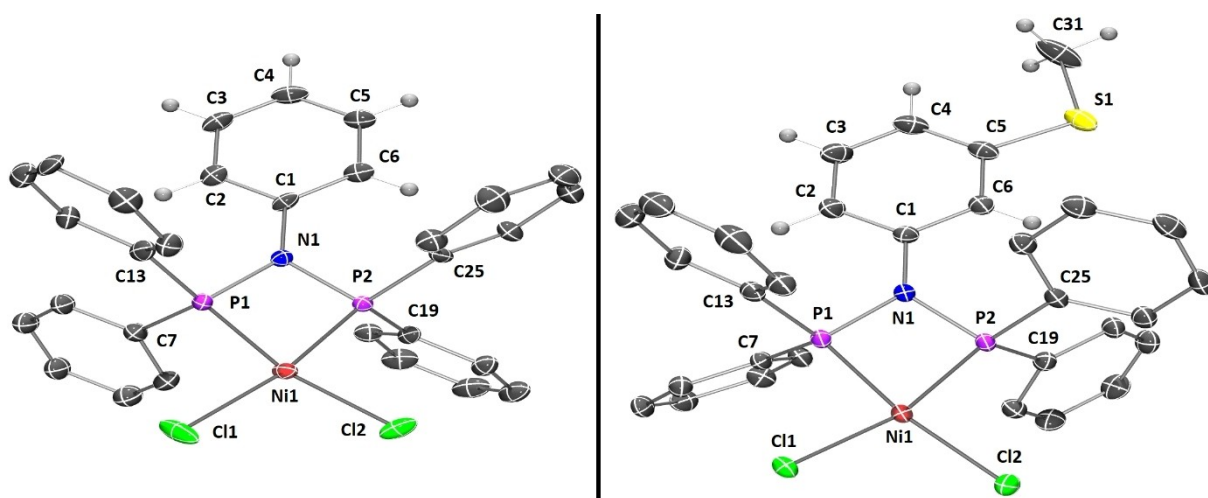


Figure 3. View of the molecular structures of complexes **12** (left) and **15** (right). Ellipsoids are represented at the 50% probability level. H atoms of the P-Ph rings are omitted for clarity. Selected bond distances (Å) and angles (deg) are listed in Table 2. ORTEP views of the asymmetric units of the crystal structures with labeling of all non-H atoms, crystal data and structure refinement parameters are available in the ESI.

13 and **14**, and they are closely related to these of **12** and **15** ($0.18 \leq \tau_4 \leq 0.19$ and $0.17 \leq \tau_4' \leq 0.18$, see ESI). Selected bond lengths and angles are summarized in Table 2, and they are in the range found in the rare examples of $[\text{NiCl}_2(\text{P},\text{N}(\text{R}),\text{P})]$ structures reported so far.^[16] The small bite-angles imposed by the diphosphine ligands result in P1-Ni1-P2 angles of $74.29(3)^\circ$ (**12**) and $74.486(18)^\circ$ (**15**), and induce a significant deformation away from the ideal square-planar geometry by opening of the Cl1-Ni1-Cl2 angles to $99.77(4)^\circ$ (**12**) and $100.359(19)^\circ$ (**15**).

By comparing the structural parameters of the palladium(II) and nickel(II) complexes reported in the present study, it can be highlighted that i) all M–P and M–Cl bond lengths are longer in the Pd^{II} complexes, as anticipated by a larger atomic radius of Pd vs. Ni, ii) the P–M–P and Cl–M–Cl angles of the Pd^{II} complexes are significantly smaller than those of their Ni^{II} analogues and iii) in contrast, the P–N–P angle is smaller in the Ni^{II} complexes (P–N and N–C bond lengths are similar in all complexes).

In each of the solid-state structures that we reported in the present contribution, *i.e.* complexes **6**, **8**- 2CHCl_3 , **12** and **15**, two anagostic C–H...M (M = Pd or Ni) intramolecular interactions ($d \approx 3.0$ - 3.2 Å), involving an *ortho*-H of two distinct *PPh* moieties could be detected (see ESI - Figure S18).

Suzuki-Miyaura Cross-Coupling Reactions

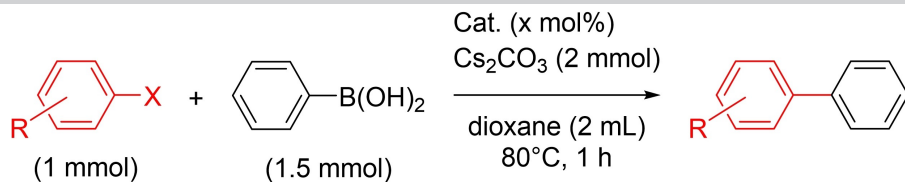

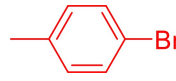
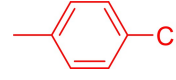
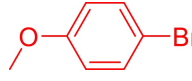
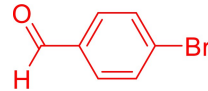
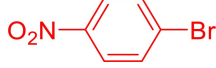
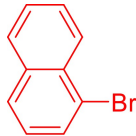
Palladium(II)-Based Catalysts

The catalytic performances of the palladium(II) complexes **6**–**10** were probed in the Suzuki-Miyaura cross-coupling reaction, using 4-bromotoluene (1 mmol) and phenylboronic acid (1.5 mmol) as model substrates (Table 3, entries 1–5). Thanks to precedent evaluations of palladium(II) complexes of *N*-substituted/functionalized DPPA-type ligands in this benchmark reaction,^[16,49, 59–65] the phase of optimization of the reaction conditions (base, solvent etc) was not necessary, and what appeared to be the optimized conditions, *i.e.* using 1 mol% catalyst, Cs_2CO_3 (2 mmol) as base, dioxane (2 mL) as solvent, and a temperature of 80°C , were applied. Within this series, complexes **6**–**9** were found to effectively mediate the cross-coupling reaction, affording the diaryl product in 88–99% yield. In contrast, complex **10**, bearing a *meta*-(C_6H_4)SMe function on the ligand backbone, was found less active, producing 4-methyl biphenyl in only 61% yield. The lower activity may therefore be attributed to steric reasons, because the other complexes possess flexible (**6**), non-functionalized (**7**) or *para*-functionalized (**8**, **9**) *N*-substituents. Since complex **6** was found to be the most performant catalyst, further tests were performed to establish the limits of catalytic system. Performing the reaction at 40°C (*vs.* 80°C) led to a drastic loss of activity, affording the coupling product in only 17% yield (Table 3, entry 6). In contrast, lowering the catalyst loading by a factor of 10, using 0.1 mol% (*vs.* 1 mol%), did not affect the yield of the reaction (Table 3, entry 7). However, reducing again the amount of complex **6**, from 0.1 mol% to 0.05 mol%, led to a slight decrease in yield to 80% (Table 3, entry 8). Using 4-chlorotoluene instead

of 4-bromotoluene as substrate led unfortunately to no conversion of the starting material (Table 3, entry 9). Altogether, these results led us to evaluate this series of complexes, with a catalyst loading of 0.1 mol% and at 80°C , towards different aryl bromides. The good results obtained with 4-bromotoluene, a substrate possessing a weak *para*-Me electron donating group (EDG), led us to evaluate a substrate with a strong *para*-OMe EDG. The catalytic activity of all complexes was strongly affected by this modification and the resulting product yields drastically dropped (Table 3, entries 10–12 and 14–15). Complex **6** still performed better than its *N*-aryl analogues, affording the coupling product in 34% yield (Table 3, entry 10), and complexes **8** and **10** exhibited the lower activities (Table 3, entries 12 and 15, respectively). Increasing the catalyst loading from 0.1 to 1 mol% allowed to reach higher yields, as observed for complex **10**, for which the yield of the coupling product jumped from 9% to 68% (Table 3, entries 15 and 16). Moving to a bromoaryl substrate possessing the moderate *para*-CHO electron withdrawing group (EWG) led to excellent product yields ($>98\%$) for all complexes (Table 3, entries 17–21). However, the product yields clearly dropped when the bromoaryl substrate is functionalized by the strong *para*-NO₂ EWG, and the results are again (as for the strong *para*-OMe EDG) dependent of the catalyst (Table 3, entries 22, 23, 25, 27, 28). While complexes **6** and **9** led to *ca.* 45% yield (Table 3, entries 22 and 27), complexes **8** and **10** led to 12 and 5% yield, respectively (Table 3, entries 25 and 28). For the worst performing systems, the product yields obtained with 0.1 mol% catalysts (5–22%, Table 3, entries 23, 25, 28) could again be improved by increasing this amount to 1 mol% (89–>99%, Table 3, entries 24, 26, 29). The catalytic activities of the palladium(II) complexes **6**–**10** were also evaluated towards the bulkier 1-bromonaphthalene substrate (Table 3, entries 30–35). The yields obtained for complexes **6** (47%), **7** (20%), **8** (<1%) and **9** (37%) were found to follow the trend of activities generally observed for the other substrates (Table 3, entries 31–34). However, complex **10**, which is generally one of the worst performing catalysts afforded in this case the coupling product with the highest yield (49%, Table 3, entry 35). As observed previously, increasing the catalyst loading, from 0.1 to 1 mol%, allowed to reach complete conversion and $>99\%$ yield of the coupling product (test realized for complex **6**, as representative example, Table 3, entry 35). For comparison, the catalytic activity of the $[\text{PdCl}_2(\text{dppm})]$ complex,^[66] supported by the commercially available dppm (dppm = bis(diphenylphosphino)methane) ligand, was evaluated towards 1-chloronaphthalene and 1-bromonaphthalene as substrates. Very low yields (<5%) were obtained (see ESI - Table S5, entries 1 and 2), highlighting the superiority of *N*-substituted DPPA-type ligands in the Pd-catalyzed Suzuki-Miyaura cross-coupling reactions.

In summary of this section, it can be highlighted that this series of palladium(II) complexes of *N*-substituted/functionalized DPPA-type ligands (**6**–**10**) are effective catalysts for the Suzuki-Miyaura cross-coupling reaction between phenylboronic acid and aryl bromides functionalized with weak and moderate EDGs and EWGs. However, their activities strongly dropped for

Table 3. Suzuki-Miyaura cross-coupling reactions catalyzed by the palladium(II) complexes (6-10) and aryl halide scope.^a

Entry	Ar-X	Cat.	x (mol%)	Yield (%) ^b
				
1		6	1	> 99
2		7	1	88
3		8	1	95
4		9	1	96
5		10	1	61
6			6	1 ^c
7	6		0.1	> 99
8	6		0.05	80
9		6	1	0
10		6	0.1	34
11		7	0.1	12
12		8	0.1	3
13		8	1	31
14		9	0.1	15
15		10	0.1	9
16		10	1	68
17		6	0.1	98
18		7	0.1	98
19		8	0.1	> 99
20		9	0.1	98
21		10	0.1	> 99
22		6	0.1	45
23		7	0.1	22
24		7	1	89
25		8	0.1	12
26		8	1	> 99
27		9	0.1	42
28		10	0.1	5
29		10	1	91
30			6	1
31	6		0.1	47
32	7		0.1	20
33	8		0.1	< 1
34	9		0.1	37
35	10		0.1	49

^a Details of the procedure are described in the Experimental Section. ^b Yields of coupling product determined by GC-FID and/or ¹H NMR in CDCl₃ analysis using hexamethylbenzene or dodecane as internal standard. Representative yields from independent experiments (at least two). ^c Reaction temperature, 40°C.

aryl bromides functionalized with strong EDGs and EWGs. Noteworthy, for the more challenging substrates and/or to improve unsatisfactory yields, an increase of catalyst loading, from 0.1 to 1 mol%, is generally needed and sufficient to reach much more appreciable yields. In the literature, the pool of palladium complexes of DPPA-type ligands applied to Suzuki-Miyaura cross-coupling and the scope of substrates studied are quite limited, therefore comparison with the present systems is also limited, but generally the latter are as good as or much better than previously reported systems.^[16] However, from the literature it can be found that the use of more sophisticated phosphine ligands allows to still diminish the catalyst loading (≤ 0.02 mol%),^[67] and/or perform the coupling reaction at room temperature.^[68–69] Complex **6**, in which the N atom is functionalized by a flexible $-(\text{CH}_2)_3\text{SMe}$, is generally outperforming its *N*-aryl analogues, and the *para*-OMe (**8**) and *meta*-SMe (**10**) derivatives are generally the less performant systems. We attempted to rationalize these differences in activity by analyzing more in details stereo-electronic differences between the ligands applied in this study. From an electronic point of view, we have highlighted that ligand **1** exhibits a slightly stronger donor ability than ligands **2–5** (see above, discussion about phosphorus-selenide coupling constant). To analyze steric factors, topographic steric maps were calculated for the complexes for which the X-ray structures were available, *i.e.* **6** and **8**, and are depicted in Figure 4 (see ESI for details).^[70–71] From this analysis, we can observe that the metal center in complex **6** is slightly more accessible, with a $\%V_{\text{Bur}}$ ca. 2% lower than complex **8**, and present a more favorable, less encumbered side (NW and NE quadrants in Figure 4a) for the approach of the substrate, while the bulkiness of the ligand is more homogeneously distributed around the metal in complex **8**. Altogether, these analyses led us to propose that, within the family of DPPA-type ligands, more basic and less-encumbered ones give the best results in Pd-catalyzed Suzuki-Miyaura cross-coupling reaction.

Nickel(II)-Based Catalysts

Considering the potential of nickel-based catalysts as sustainable alternative to palladium ones,^{see e.g. [69,72–74]} we evaluated the Ni^{II} complexes reported therein towards the Suzuki-Miyaura cross-coupling reaction to obtain a direct comparison with their Pd^{II} analogues. It is noteworthy that, although several nickel complexes of *N*-substituted/functionalized DPPA-type were already reported, their application in cross-coupling reactions remains scarce.^[17] Indeed, only a few reports mention their use in Kumada coupling reaction,^[75–77] and to the best of our knowledge, solely the $[\text{NiCl}_2(\text{P},\text{P})]$ ($\text{P},\text{P}=(\text{Ph}_2\text{P})_2\text{N}-\text{S}-\text{CHMePh}$) complex was evaluated in Suzuki-Miyaura cross-coupling reaction, and it was found (nearly) inactive ($< 1\text{--}5\%$ yield under the studied conditions).^[75]

A preliminary test, consisting in simply replacing a Pd-catalyst by its Ni analogue into the catalytic mixture and applying the optimized (for Pd) reaction conditions (2 mmol Cs_2CO_3 as base, 2 mL dioxane, 1 h, 80 °C, see Table 3), was realized with complexes **11** and **14**. For both complexes, the cross-coupling reaction between 4-bromotoluene and phenylboronic acid as model substrates was attempted, using 1 mol% of Ni-based catalyst, but no conversion was observed. No conversion was also observed using $[\text{NiCl}_2(\text{dppm})]$ ^[78] as precatalyst (see ESI - Table S5, entries 3 and 4). Direct comparison of the performances of the Pd vs. Ni catalysts could therefore not be done under these conditions.

Recent studies by Han and coworkers^[79] and Garg and coworkers^[40] were found of importance for the present work, because the authors studied Ni catalysts of the type $[\text{NiCl}_2(\text{P},\text{P})]$ ($\text{P},\text{P}=\text{dppe}$, $(\text{PCy}_3)_2$), a scaffold very similar to the complexes studied therein, for the cross-coupling of aryl halides and aryl boronic acids. On the basis of these studies, a more general literature survey and the motivation to use as much as possible “green” reagents and in the lowest quantities, we decided to evaluate our series of Ni^{II} complexes (**11–15**) towards the cross-coupling reaction between 1-bromo- or 1-chloronaphthalene (1 mmol) and phenylboronic acid (1.2 mmol), using a low (for Ni) catalyst loading of 1 mol%, K_3PO_4 (2 mmol) as a non-toxic, inexpensive and readily available base and *tert*-amyl alcohol (*t*AA, 2 mL) as a green solvent (see Table 4). Under these

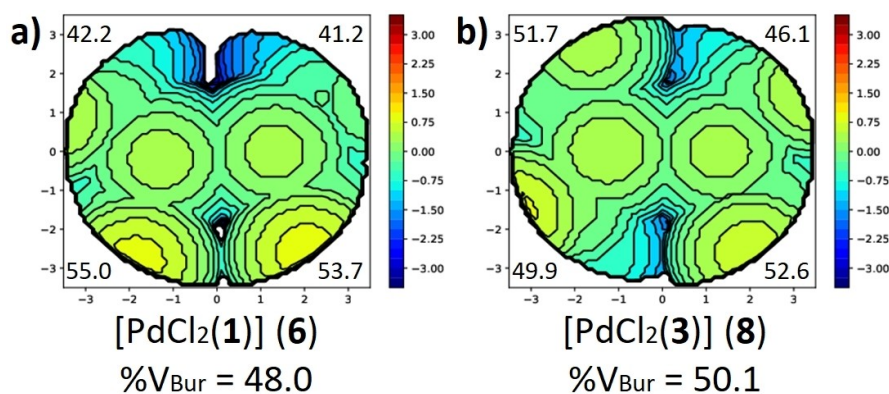


Figure 4. Buried volume parameter ($\%V_{\text{Bur}}$) and topographic steric maps of catalysts **6** (a) and **8** (b) showing $\%V_{\text{Bur}}$ by quadrant (see ESI for more details).

Table 4. Evaluation of the nickel(II) complexes (11–15) in the Suzuki–Miyaura cross-coupling reaction between 1-bromo- and 1-chloronaphthalene and phenylboronic acid.^a

Entry	Cat.	X	Yield (%) ^b
1	11	Br	98
2	12	Br	62
3	13	Br	44
4	14	Br	66
5	15	Br	63
6	11	Cl	90
7	12	Cl	92
8	13	Cl	88
9	14	Cl	85
10	15	Cl	65

^a Details of the procedure are described in the Experimental Section. ^b Yields of coupling product determined by GC-FID using hexamethylbenzene as internal standard. Representative yields from independent experiments (at least two). tAA = *tert*-amyl alcohol.

reaction conditions, our series of catalysts efficiently mediated the aforementioned reaction, at 100 °C over 8 h, and afforded the corresponding coupling products in good to excellent yields (Table 4). Surprisingly, the reactions with 1-chloronaphthalene led to similar or even higher yields (65–92%, Table 4, entries 6–10) than this with 1-bromonaphthalene (44–98%, Table 4, entries 1–5), while the latter are generally more reactive for this type of cross-coupling reactions. It can be noticed that in all reactions, the total amount of consumed naphthyl halide was converted into the coupling product, and no homo-coupling by-product could be detected by GC-FID. Complex 11 afforded the 1-phenylnaphthalene coupling product in 98% and 90% yield from 1-bromonaphthalene (Table 4, entry 1) and 1-chloronaphthalene (Table 4, entry 6), respectively, and it was therefore selected to extend the scope of aryl halides and aryl boronic acids (see below). For a comparison purpose, under these catalytic reaction conditions, the [NiCl₂(dppm)] precatalyst led to comparable results for 1-bromonaphthalene (75% yields, see ESI - Table S5, entry 8, vs. 44–98 for 11–15), but was found much less effective towards 1-chloronaphthalene (50% yields, see ESI - Table S5, entry 7, vs. 65–92 for 11–15).

As for the palladium-based catalysts, we attempted to rationalize the differences in activity between the different nickel (pre)catalysts by analyzing the stereo-electronic variations between the studied ligands/complexes. Of course, ligand 1 still presents a slightly stronger donor ability than ligands 2–5 (see above, discussion about phosphorus-selenide coupling constant). Analysis of steric factors *via* the calculation of topographic steric maps^[70–71] for the whole series of nickel complexes (11–15) revealed very similar %V_{Bur} for complexes 11 and 13–15 (51.3–51.9), while the %V_{Bur} of 12 was found slightly

larger (53.2) (ESI for details and Figure S19). Concerning the distribution of the bulkiness by quadrant, this of complex 13 is quite homogeneous, while these in the other complexes exhibit always either a less bulky face (W in 12) or diagonal (NE/SW in 11 and 15, NW/SE in 14). Altogether these observations concerning the stereo-electronic properties of the ligands/complexes do not allow to rationalize the observed trend in catalysis, with complex 11 clearly outperforming its analogues 12–15.

Under the optimized conditions (see Table 4), complex 11 readily mediated the cross-coupling of phenylboronic acid with an array of aryl halides (Figure 5). While no general trend emerged from these results, it can be highlighted that complex 11 is especially efficient for the coupling of diaryl halides (≥ 90% for 2-bromo- and 1-bromo-/chloro-naphthalene) and aryl halides *para*-functionalized with some strong EWGs (–C(O)Me, –C(O)OH or –CN groups) (Figure 5). Aryl halides bearing other EDGs and EWGs, such as –Me, –OMe and –NO₂, –F, –CF₃, respectively, gave more modest results (15–54% yields, Figure 5). It should be noticed that the reported system is tolerant to *ortho*-functionalization (14% yield for 2-bromoanisole) and allows the coupling of halo-heterocycles with variable efficiency (99% for 3-bromopyridine and *ca.* 25% for 2-chloro- and 2-bromo-pyridine). No conversion was observed when 2-amino-3-bromopyridine was used as substrate, probably due to the interference of the amino group with the catalyst.

The applicability of our system to the coupling of various aryl boronic acids, substituted with both EWGs and EDGs, was studied, under the optimized conditions, with 1-bromonaphthalene as electrophile (Figure 6). While the substitution pattern on the aryl halide substrates was found to strongly affect the

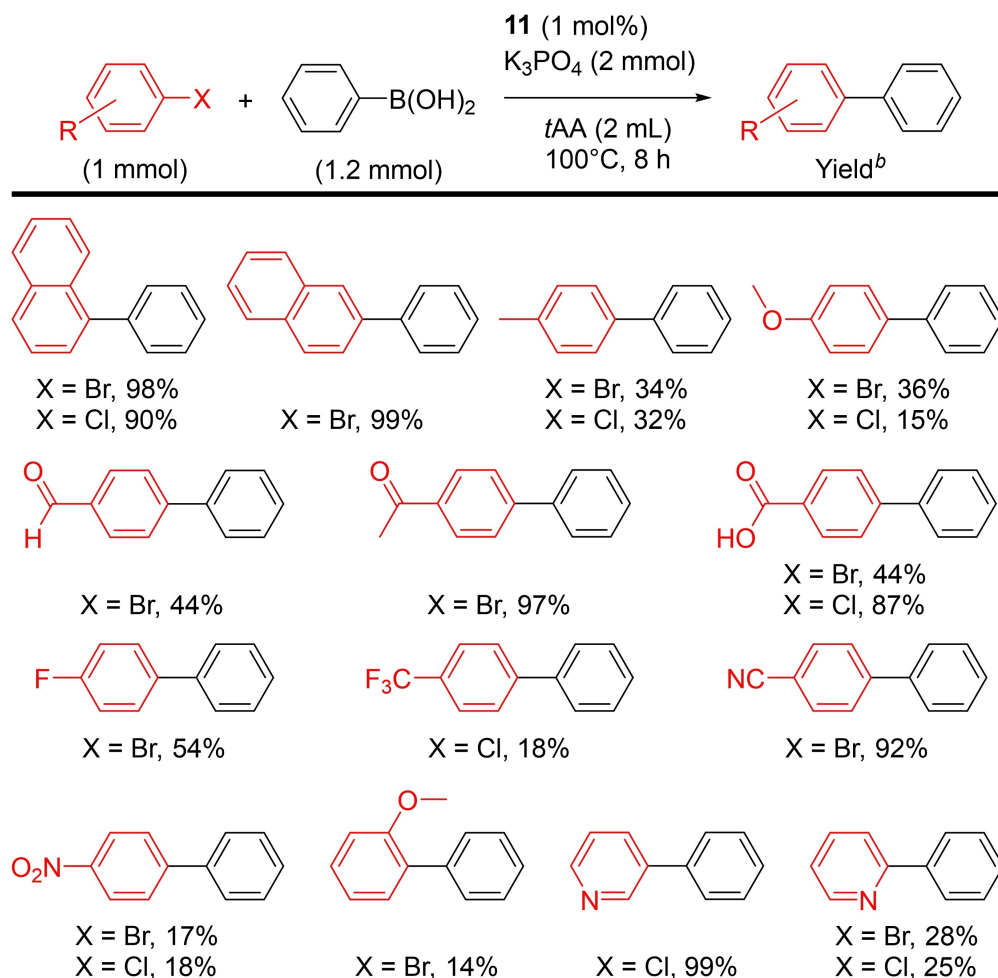


Figure 5. Suzuki-Miyaura cross-coupling of various aryl halides and phenylboronic acid.^{ab}

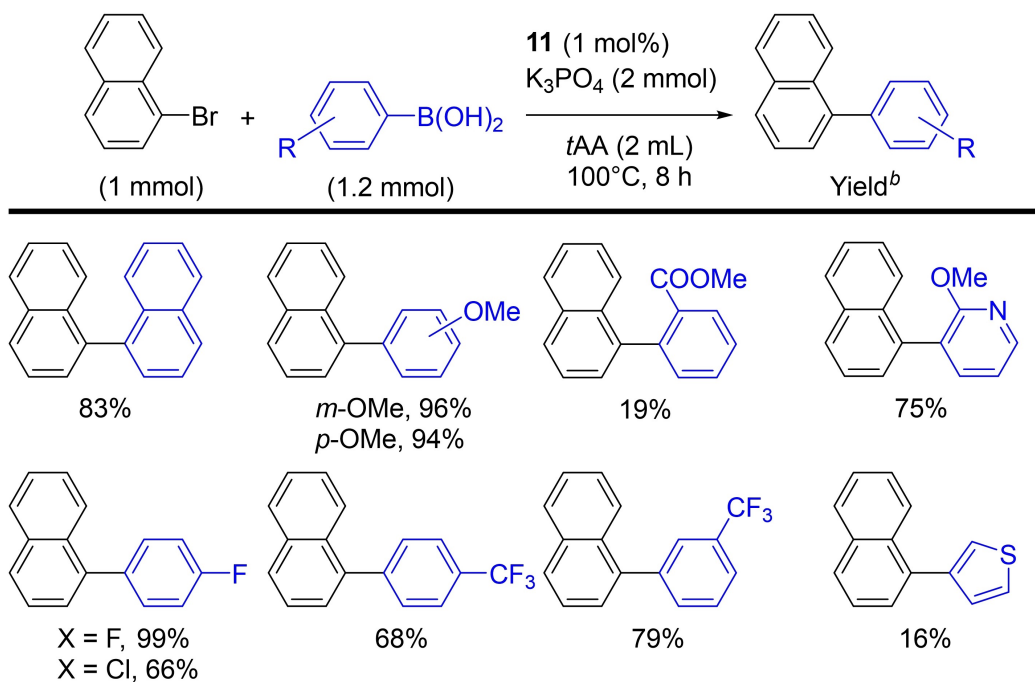


Figure 6. Suzuki-Miyaura cross-coupling of 1-bromonaphthalene with various aryl boronic acids.^{ab}

yield of the corresponding coupling products (see Figure 5), such effect was not observed by varying the functionalization of the aryl boronic substrates. Indeed, the coupling of 1-bromonaphthalene with aryl boronic acids functionalized with the strong electron donating methoxy group, both in *para* or *meta* positions, afforded the corresponding coupling products in very high yields (94 and 96%, respectively, Figure 6). Similarly, the presence of strong EWGs, such as F, Cl, CF₃ (*para* or *meta*) did not inhibit the cross-coupling reaction, and good to excellent yields were obtained (66–99%, Figure 6). The synthesis of 1,1'-binaphthalene could also be achieved in 83% yield, however the presence of a relatively bulky and strong EWG, such as an ester group, in *ortho* position induced a drop in the yield of the coupling product to 19%, which was therefore attributed to the steric constraint (Figure 6).

In summary of this section, it can be highlighted that this series of nickel(II) complexes of *N*-substituted/functionalized DPPA-type ligands (11–15) are effective catalysts for the Suzuki-Miyaura cross-coupling reaction between aryl bromides and aryl chlorides, although the nature of the EDGs or EWGs may affect the product yields, and a wide range of aryl boronic acids bearing both EDGs and EWGs. The “classical” reaction conditions used for palladium-based catalysts, *i.e.* Cs₂CO₃/dioxane, totally inhibit these catalysts. However, adaptation to greener reaction conditions, *i.e.* K₃PO₄/tAA, revealed the high potential of these complexes towards the targeted application. Although no direct comparison can be made with similar systems, because complexes 11–15 are the first examples of nickel complexes supported by DPPA-type ligands active in Suzuki-Miyaura cross-coupling reaction, the activities of the latter are comparable to many other reported systems.^[69,80–81]

Additional Catalytic Reactions

In the light of the interesting results obtained with the nickel complexes 11–15 (see above), which were accessed under greener reaction conditions than those usually applied to palladium complexes of *N*-substituted DPPA-type ligands, we wondered if their palladium analogues 6–10 would also be effective in the Suzuki-Miyaura cross-coupling reaction under these reaction conditions. It may be important to recall that the nickel complexes were not active under the reaction conditions

applied to the palladium ones. Therefore, we selected complex 6, as the best performing catalyst, four different aryl halides and phenylboronic acid, as substrates, to evaluate the ability of our Pd-based catalysts to mediate the Suzuki-Miyaura cross-coupling reaction under the “green” reaction conditions successful for the Ni-based catalysts (see Figure 7). First of all, the excellent yields recorded for the reactions using 4-bromotoluene (99%) and 1-bromonaphthalene (99%) allowed us to establish that these reaction conditions were not detrimental to our system, because they were similar to those obtained with the classical reaction conditions (see Figure 7 and Table 3 for comparison). Moreover, while complex 6 was found inactive for the coupling of 4-chlorotoluene and phenylboronic acid when combined with Cs₂CO₃ in dioxane at 80 °C (Table 3, entry 9), it afforded 7% of the coupling product using K₃PO₄ in tAA at 100 °C (Figure 7). For comparison purpose, the reaction with 1-chloronaphthalene was also attempted and afforded 28% yield of the coupling product (Figure 7). The two latter results highlight that, although the product yields remain lower than with the Ni-based catalysts, applying alternative reaction conditions than those typically employed allowed to realize the coupling of aryl chlorides, which was never reported for palladium complexes of *N*-substituted DPPA-type complexes.^[16,49,59–65] Additionally, using [PdCl₂(dppm)] as precatalyst under these reaction conditions, similar yield was obtained for 1-bromonaphthalene (99%), but no conversion was observed for 1-chloronaphthalene (see ESI - Table S5, entries 5 and 6), highlighting again the superiority of *N*-substituted DPPA-type ligands.

A control of the stability of both palladium and nickel complexes in *tert*-amyl alcohol revealed that; i) all complexes are only scarcely soluble in this solvent and do not present any trace of degradation after 12 h at room temperature (see ESI - Figures S20 and S21), and ii) while the nickel complexes do not degrade after heating for 8 h at 100 °C (see ESI - Figures S21), the palladium complexes partially degrade (formation of grey powder, see ESI, Figures S20). The greater stability of the nickel complexes may contribute to their higher activity towards chlorinated substrates. Moreover, similarly to the work of Shi and coworkers,^[82] we ran a series of experiments that highlighted the requirement of both the base (K₃PO₄) and the boronic acid to “activate” the catalyst, presumably *via* the formation of Ni⁰ active catalytic species (see ESI - Figures S22).

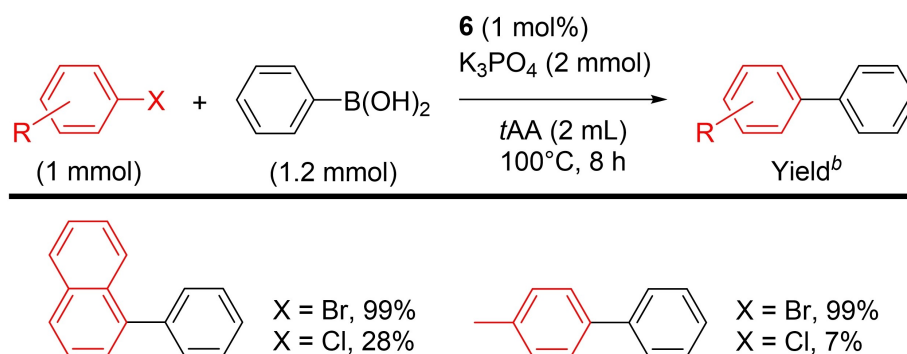


Figure 7. Suzuki-Miyaura cross-coupling reactions catalyzed by the palladium(II) complex (6) under “greener” reaction conditions.^{a,b}

Conclusions

In the present contribution, we reported one new *N*-functionalized DPPA-type ligand, three new palladium(II) and two new nickel(II) complexes of such ligands, which were thoroughly characterized, both in solution and in the solid-state. X-ray diffraction studies allowed to confirm the anticipated structures for four of the five new complexes. The access of such complexes is very efficient (most of the yields are >80%) and straightforward, because it requires only two steps; one for the ligand synthesis, from the corresponding amine, and one for the complexation. All complexes are air stable. Newly synthesized and previously reported complexes constitute two series of bench-stable palladium(II) (6-10) and nickel(II) (11-15) complexes that were further evaluated in the Suzuki-Miyaura cross-coupling reaction. Palladium(II) complexes (6-10) were found to be effective catalysts for the Suzuki-Miyaura cross-coupling reaction between phenylboronic acid and aryl bromides functionalized with weak and moderate EDGs and EWGs, using as low as 0.1 mol% catalyst, in combination with Cs₂CO₃ in dioxane at 80 °C within 1 h. However, their activities strongly dropped for aryl bromides functionalized with strong EDGs and EWGs, and no activity was recorded for aryl chlorides. Nickel(II) complexes (11-15) were initially evaluated under similar reaction conditions, but did not exhibit any catalytic activity. However, by tuning the reaction conditions, using K₃PO₄ as a non-toxic, inexpensive and readily available base and *tert*-amyl alcohol as a green solvent (100 °C, 8 h), the potential of these nickel catalysts was revealed and clearly outperformed their palladium analogues in some instances, for example by converting aryl chlorides up to 90%. Interestingly, these reaction conditions could also be applied to the palladium-based catalysts, improving their efficiency towards aryl chlorides (up to 28% yield vs. 0%) and not affecting their performances towards aryl bromides. The nickel-catalyzed Suzuki-Miyaura cross-coupling reaction, with *N*-substituted DPPA-type ligands, features a broad substrate scope (aryl halides and aryl boronic acids), applicability under green reaction conditions, and operational simplicity (air stable complexes), several arguments that make it a viable alternative to its palladium predecessor. Within both Pd and Ni series of precatalysts, these supported by ligand **1**, *i.e.* complexes **6** and **11**, respectively, were found to be the most efficient. Generally, both the palladium(II) and nickel(II) systems based on *N*-substituted DPPA-type ligands are outperforming their analogues supported by the common dppm ligand. Stereo-electronic parameters of the ligands/complexes were investigated to attempt to rationalize this behavior, and it was tentatively concluded that the superiority of ligand **1** may arise from its strongest donor ability and to a lower %V_{Bur}. Further mechanistic investigations, both experimentally and computationally, are planned to get more insight between the difference in catalytic activities between the Pd- and Ni-based systems reported in the present contribution.

Experimental Section

Materials and Instrumentation

General. All manipulations were conducted under an inert gas (argon) atmosphere, using Schlenk-line techniques or in an argon-filled glovebox, in flame-dried glassware. Aniline (99%, Sigma Aldrich), 3-(methylthio)aniline (97%, Sigma Aldrich), 4-(methylthio)aniline (97%, Sigma Aldrich), 4-methoxyaniline (99%, Sigma Aldrich), 3-(methylthio)propylamine (97%, Sigma Aldrich), chlorodiphenylphosphine (>97%, TCI Chemicals), triethylamine (≥99.4%, Thermo Scientific Chemicals), bis(acetonitrile)dichloropalladium(II) ([PdCl₂(CH₃CN)₂], 99%, Sigma Aldrich), phenylboronic acid (≥97%, Sigma Aldrich), 1-naphthylboronic acid (≥95%, Sigma Aldrich), 4-chlorophenylboronic acid (95%, Sigma Aldrich), 4-fluorophenylboronic acid (≥95%, Sigma Aldrich), 4-(trifluoromethyl)phenylboronic acid (≥95%, Sigma Aldrich), 3-(trifluoromethyl)phenylboronic acid (≥95%, Sigma Aldrich), 4-methoxyphenylboronic acid (≥95%, Sigma Aldrich), 3-methoxyphenylboronic acid (97%, Thermo Scientific Chemicals), 2-methoxy-carbonylphenylboronic acid (≥95%, Sigma Aldrich), 4-bromotoluene (98%, Sigma Aldrich), 4-chlorotoluene (98%, Sigma Aldrich), 4-bromobenzaldehyde (99%, Sigma Aldrich), 4'-bromoacetophenone (98%, Sigma Aldrich), 4-bromobenzoic acid (98%, Sigma Aldrich), 4-chlorobenzoic acid (99%, Sigma Aldrich), 1-bromo-4-nitrobenzene (99%, Sigma Aldrich), 1-chloro-4-nitrobenzene (99%, Sigma Aldrich), 4-bromoanisole (≥99%, Sigma Aldrich), 4-chloroanisole (99%, Sigma Aldrich), 1-bromonaphthalene (≥95%, Sigma Aldrich), 1-chloronaphthalene (>97%, TCI Chemicals), 1-bromo-4-fluorobenzene (99%, Sigma Aldrich), 1-bromo-4-(trifluoromethyl)benzene (>98%, TCI Chemicals), 4-bromobenzonitrile (99%, Sigma Aldrich), 1-bromo-2-methoxybenzene (97%, Sigma Aldrich), 2-chloropyridine (99%, Sigma Aldrich), hexamethylbenzene (99%, Sigma Aldrich) and dodecane (≥99%, Sigma Aldrich) were used as received. Reagent grade tetrahydrofuran, dichloromethane, pentane and diethyl ether were purchased from Carlo Erba and purified using an MBraun SPS system. Dimethoxyethane (DME) was distilled over sodium/benzophenone. 1,4-Dioxane (>99%, TCI Chemicals), *tert*-amyl alcohol (>98%, TCI Chemicals), CD₂Cl₂ and CDCl₃ (99.8% D, Eurisotop) were degassed and stored on 4 Å molecular sieves (Fluka) prior to use. Complexes [NiCl₂(DME)]^[83] **11**,^[26] **13**^[52] and **14**^[24] were prepared according to previously reported methods.

Characterisations. All NMR spectra were recorded on a Bruker Avance III 300 or 400 MHz spectrometer at ambient temperature. ¹H and ¹³C chemical shifts (δ) are reported in ppm vs. SiMe₄ and were determined using the residual ¹H and ¹³C solvent peaks as internal standards. The coupling constants are reported in Hertz. "*J*_{C-P}": separation between the most intense and one adjacent lines in the observed "virtual triplets" in the "virtually coupled" ¹³C{¹H} AA'X subspectra (A, A' = ³¹P; X = ¹³C). The IR spectra were recorded in the 4000–600 cm⁻¹ region on a PerkinElmer Frontier FT-IR spectrometer (ATR mode, diamond crystal). The elemental analyses were carried out by the analytical service of the LCC-Toulouse by using a PerkinElmer 2400 CHNS/O Series II System (100 V). The electrospray ionization mass spectra (ESI-MS) were recorded by the ICT service of Paul Sabatier University Toulouse III on a Q-ToF Premier (Waters) instrument using nitrogen as drying agent and nebulizing gas and MeCN as solvent. After treatment (see below), the catalytic reactions were analysed by gas chromatography on an Agilent 7820 A chromatograph equipped with a FID detector, a DB-WAX capillary column (30 m × 0.32 mm × 0.5 μm) and autosampler or on a Shimadzu GC 2014 chromatograph equipped with a FID detector, a SLB 5 ms capillary column (30 m × 0.32 mm × 0.23 μm) and autosampler. Authentic samples of reactants and products were used for calibration. The conversion of starting material and the

yield of the cross-coupling product were calculated from the calibration curves ($r^2=0.999$) and an internal standard (hexamethylbenzene). In some cases, conversion and yield were also determined by ^1H NMR analysis using hexamethylbenzene or dodecane as internal standards. Due to solubility issues, $^{13}\text{C}\{^1\text{H}\}$ NMR spectra of some palladium(II) and nickel(II) complexes are incompletely or not described. Ligand **5** was not obtained in an analytically pure form, and was therefore used as obtained for the complexation reaction (see details below).

X-ray structural analyses. Single crystal of each compound was mounted under inert perfluoropolyether at the tip of a glass fiber and data were collected on either a Bruker APEXII diffractometer using MoK α radiation for **6** and **8**, or a Rigaku XtaLAB Synergy Dualflex diffractometer using a PhotonJet X-ray source (CuK α , $\lambda=1.54184$ Å) for **12** and **15**. An Oxford Cryosystems Cryostream cooling device was used to collect data at low temperature (100(2) K). Omega scans were performed for data collection. An empirical absorption correction was applied and the structures were solved by using the integrate space-group and crystal structure determination SHELXT^[84] software and all non-hydrogen atoms were refined anisotropically by means of least-squares procedures on F^2 using SHELXL-2014.^[85] All H atoms attached to carbon atoms were introduced in the calculations at idealised positions and treated according to the riding model. In compound **8**, there are two CHCl_3 solvent molecules by asymmetric unit. In compound **12** all phenyl rings are disordered over two positions. These disorders are refined using the PART and SAME instructions within SHELXL. The drawing of the molecules were realised with the help of ORTEP32,^[86-87] and POV-Ray version 3.7. ORTEP views of the asymmetric units of the crystal structures with labeling of all non-H atoms, and tables giving crystal data and structure refinement parameters are available in the ESI.

Synthesis of Ligand 5

Chlorodiphenylphosphine (6.342 g, 28.73 mmol) was added dropwise to a solution of 3-(methylthio)aniline (2.000 g, 14.37 mmol) and triethylamine (3.631 g, 35.91 mmol) in 150 mL of THF under an inert atmosphere. The reaction mixture was stirred for 3 h. After filtration, the volatiles were removed under reduced pressure and the residue was washed twice with pentane to give **5** as a colorless solid. Ligand **5** was not obtained in an analytically pure form; its purity was evaluated at 90% from NMR. However, the residual impurities did not affect the coordination process with the metal precursor. Therefore, it was used as obtained for complexation, and the impurities could be eliminated during the purifications of corresponding metal complexes **10** and **15** (see below). Only the $^{31}\text{P}\{^1\text{H}\}$ NMR and ESI-MS spectra are reported for **5**. $^{31}\text{P}\{^1\text{H}\}$ NMR (CD_2Cl_2 , 121.5 MHz): δ 69.02 (s) ppm. MS (ESI): m/z 508.1 $[\text{M} + \text{H}]^+$.

General Procedure for the Synthesis of Bis-Selenide Phosphine Ligands

In the glovebox, to a 4 mL vial containing a magnetic stirring bar were added **1** (0.021 mmol, 10 mg, 1.0 eq), grey selenium powder (5.0 mg, 0.055 mmol, 2.6 eq) and dry CDCl_3 (1 mL). After 24 hours, the obtained dark mixture was analyzed by $^{31}\text{P}\{^1\text{H}\}$ NMR analysis to confirm the formation of the desired compound **1- Se_2** .

This procedure was repeated for the synthesis of the others bis-selenide phosphine ligands **2- Se_2** -**5- Se_2** , and all data are summarized in Table 1.

Synthesis of the Palladium(II) Complexes

Synthesis of 6

To a suspension of $[\text{PdCl}_2(\text{CH}_3\text{CN})_2]$ (54.7 mg, 0.211 mmol) in CH_2Cl_2 (10 mL) was added a solution of **1** (0.100 g, 0.211 mmol) in CH_2Cl_2 (10 mL). The solution quickly turned yellow and was stirred at room temperature for 4 h. The solvent was removed under reduced pressure, and the resulting pale-yellow solid was washed with pentane (2 x 10 mL). Light yellow crystals suitable for single-crystal X-ray diffraction studies were grown by slow diffusion of pentane into a saturated CH_2Cl_2 solution of **6**. Yield: 122 mg, 89%. Anal. Calcd for $\text{C}_{28}\text{H}_{29}\text{Cl}_2\text{NP}_2\text{PdS}$ (650.87): C, 51.67; H, 4.49; N, 2.25. Found: C, 51.57; H, 4.51; N, 2.25. FTIR: $\nu_{\text{max}}(\text{solid})/\text{cm}^{-1}$ 3051 w, 2200 w, 1583 w, 1571 w, 1478 w, 1455 w, 1434 s, 1418 w, 1307 w, 1224 m, 1185 w, 1163 w, 1135 s, 1100 s, 1068 m, 1024 w, 995 m, 959 w, 856 s, 818 w, 752 s, 719 m, 695 s, 615 w. ^1H NMR (CD_2Cl_2 , 300 MHz): δ 7.87-7.94 (m, 8H, H_{meta} of Ar), 7.69-7.75 (m, 4H, H_{para} of Ar), 7.58-7.63 (m, 8H, H_{ortho} of Ar), 3.11-3.28 (m, 2H, NCH_2), 2.05 (t, 2H, $^3J_{\text{H,H}}=6.6$ Hz, CH_2S), 1.76 (s, 3H, SCH_3), 1.26-1.36 (m, 2H, $\text{CH}_2\text{CH}_2\text{CH}_2$) ppm. $^{13}\text{C}\{^1\text{H}\}$ NMR (CD_2Cl_2 , 75.5 MHz): δ 134.03 (AA'X virtual t, $J_{\text{C,P}}=6.7$ Hz, C-H arom), 133.95 (AA'X virtual t, $J_{\text{C,P}}=1.5$ Hz, C-H arom), 129.94 (AA'X virtual t, $J_{\text{C,P}}=1.3$ Hz, C-H arom), 48.60 (s, NCH_2), 31.24 (s, CH_2S), 28.06 (s, $\text{CH}_2\text{CH}_2\text{CH}_2$), 15.49 (s, SCH_3), C_{quat} not observed. $^{31}\text{P}\{^1\text{H}\}$ NMR (CD_2Cl_2 , 121.5 MHz): δ 31.01 (s) ppm. MS (ESI): m/z 616.00 $[\text{M} - \text{Cl}]^+$, 634.00 $[\text{M} - \text{Cl} + \text{H}_2\text{O}]^+$.

Synthesis of 7

The same procedure was used with $[\text{PdCl}_2(\text{CH}_3\text{CN})_2]$ (56.2 mg, 0.217 mmol) and **2** (0.100 g, 0.217 mmol). Yield: 130 mg, 94%. Anal. Calcd for $\text{C}_{30}\text{H}_{25}\text{Cl}_2\text{NP}_2\text{Pd}$ (638.80): C, 56.41; H, 3.94; N, 2.19. Found: C, 56.48; H, 4.01; N, 2.23. FTIR: $\nu_{\text{max}}(\text{solid})/\text{cm}^{-1}$ 3050 w, 2985 w, 1588 m, 1596 m, 1492 m, 1480 m, 1455 w, 1436 s, 1314 w, 1283 w, 1245 s, 1185 w, 1162 m, 1106 s, 1095 s, 1025 m, 995 m, 982 w, 948 s, 911 s, 886 m, 760 m, 752 s, 744 s, 721 m, 698 m, 686 s, 617 w. ^1H NMR (CD_2Cl_2 , 400 MHz): δ 7.87-7.93 (m, 8H, H_{meta} of Ar), 7.67-7.71 (m, 4H, H_{para} of Ar), 7.52-7.57 (m, 8H, H_{ortho} of Ar), 7.16-7.20 (m, 1H, $\text{N}(\text{C}_6\text{H}_5)$, $\text{H}_{\text{para}}/\text{N}$), 7.06-7.10 (m, 2H, $\text{N}(\text{C}_6\text{H}_5)$, $\text{H}_{\text{meta}}/\text{N}$), 6.51-6.54 (m, 2H, $\text{N}(\text{C}_6\text{H}_5)$, $\text{H}_{\text{ortho}}/\text{N}$) ppm. $^{31}\text{P}\{^1\text{H}\}$ NMR (CD_2Cl_2 , 162 MHz): δ 34.30 (s) ppm.

Synthesis of 8

The same procedure was used with $[\text{PdCl}_2(\text{CH}_3\text{CN})_2]$ (52.8 mg, 0.203 mmol) and **3** (0.100 g, 0.203 mmol). Light yellow crystals suitable for single-crystal X-ray diffraction studies were grown by slow diffusion of pentane into a saturated CHCl_3 solution of **8**. Yield: 117 mg, 86%. Anal. Calcd for $\text{C}_{31}\text{H}_{27}\text{Cl}_2\text{NOP}_2\text{Pd}$ (668.83): C, 55.67; H, 4.07; N, 2.09. Found: C, 55.38; H, 4.11; N, 2.04. FTIR: $\nu_{\text{max}}(\text{solid})/\text{cm}^{-1}$ 2989 m, 2901 m, 1615 w, 1583 w, 1508 s, 1481 m, 1438 s, 1394 w, 1306 m, 1243 s, 1182 m, 1161 w, 1106 s, 1057 w, 1038 s, 1028 s, 997 m, 953 s, 920 s, 829 s, 799 m, 757 m, 748 s, 722 m, 695 s, 687 s, 635 w, 623 w. ^1H NMR (CD_2Cl_2 , 300 MHz): δ 7.83-7.91 (m, 8H, H_{meta} of Ar), 7.66-7.71 (m, 4H, H_{para} of Ar), 7.51-7.57 (m, 8H, H_{ortho} of Ar), 6.57 (AA' part of a AA'BB' spin system, 2H, $^3J_{\text{H,H}}=8.9$ Hz, $\text{N}(\text{C}_6\text{H}_4)\text{O}$, $\text{H}_{\text{meta}}/\text{N}$), 6.37 (BB' part of a AA'BB' spin system, 2H, $^3J_{\text{H,H}}=8.9$ Hz, $\text{N}(\text{C}_6\text{H}_4)\text{O}$, $\text{H}_{\text{ortho}}/\text{N}$), 3.68 (s, 3H, OCH_3) ppm. $^{31}\text{P}\{^1\text{H}\}$ NMR (CD_2Cl_2 , 121.5 MHz): δ 35.77 (s) ppm.

Synthesis of 9

The same procedure was used with $[\text{PdCl}_2(\text{CH}_3\text{CN})_2]$ (51.1 mg, 0.197 mmol) and **4** (0.100 g, 0.197 mmol). Yield: 123 mg, 91%. Anal. Calcd for $\text{C}_{31}\text{H}_{27}\text{Cl}_2\text{NP}_2\text{PdS}$ (684.89): C, 54.36; H, 3.97; N, 2.05. Found:

C, 53.90; H, 3.80; N, 2.11. FTIR: $\nu_{\max}(\text{solid})/\text{cm}^{-1}$ 2989 m, 2901 m, 1589 m, 1492 s, 1481 s, 1438 s, 1406 w, 1394 w, 1309 w, 1248 s, 1181 w, 1162 w, 1107 s, 1097 s, 1067 w, 1058 w, 1027 w, 1006 w, 982 w, 964 w, 949 s, 933 w, 912 s, 853 w, 837 w, 825 m, 813 m, 744 s, 723 m, 695 s, 686 s 631 w, 616 w. $^1\text{H NMR}$ (CD_2Cl_2 , 300 MHz): δ 7.85-7.92 (m, 8H, H_{meta} of Ar), 7.66-7.77 (m, 4H, H_{para} of Ar), 7.52-7.57 (m, 8H, H_{ortho} of Ar), 6.90 (AA' part of a AA'BB' spin system, 2H, $^3J_{\text{H,H}}=8.8$ Hz, $\text{N}(\text{C}_6\text{H}_4)\text{S}$, $\text{H}_{\text{meta}}/\text{N}$), 6.40 (BB' part of a AA'BB' spin system, 2H, $^3J_{\text{H,H}}=8.8$ Hz, $\text{N}(\text{C}_6\text{H}_4)\text{S}$, $\text{H}_{\text{ortho}}/\text{N}$), 2.36 (s, 3H, SCH_3) ppm. $^{13}\text{C}\{^1\text{H}\}$ NMR (CD_2Cl_2 , 75.5 MHz): δ 134.34 (AA'X virtual t, $J_{\text{C,P}}=6.7$ Hz, C-H arom), 133.99 (AA'X virtual t, $J_{\text{C,P}}=1.30$ Hz, C-H arom), 129.78 (AA'X virtual t, $J_{\text{C,P}}=6.3$ Hz, C-H arom), 127.38, (AA'X virtual t, $J_{\text{C,P}}=3.3$ Hz, C-H arom), 126.92 (AA'X virtual t, $J_{\text{C,P}}=1.3$ Hz, C-H arom), 15.35 (s, SCH_3), C_{quat} not observed. $^{31}\text{P}\{^1\text{H}\}$ NMR (CD_2Cl_2 , 121.5 MHz): δ 35.27 (s) ppm. MS (ESI): m/z 650.00 $[\text{M} - \text{Cl}]^+$, 668.00 $[\text{M} - \text{Cl} + \text{H}_2\text{O}]^+$.

Synthesis of 10

The same procedure was used with $[\text{PdCl}_2(\text{CH}_3\text{CN})_2]$ (51.1 mg, 0.197 mmol) and **5** (0.100 g, 0.197 mmol). Yield: 0.112 g, 83%. Anal. Calcd for $\text{C}_{31}\text{H}_{27}\text{Cl}_2\text{NP}_2\text{PdS}$ (684.89): C, 54.36; H, 3.97; N, 2.05. Found: C, 53.80; H, 3.79; N, 2.16. FTIR: $\nu_{\max}(\text{solid})/\text{cm}^{-1}$ 2989 m, 2901 m, 1586 m, 1571 m, 1479 m, 1435 s, 1313 w, 1281 m, 1241 s, 1185 w, 1161 w, 1105 s, 1097 s, 1067 w, 1058 w, 1027 w, 1008 m, 988 s, 963 s, 934 w, 916 s, 871 w, 823 m, 776 s, 747 s, 720 m, 707 sm 689 s, 679 s, 657 m, 615 w. $^1\text{H NMR}$ (CD_2Cl_2 , 300 MHz): δ 7.87-7.94 (m, 8H, H_{meta} of Ar), 7.67-7.73 (m, 4H, H_{para} of Ar), 7.53-7.59 (m, 8H, H_{ortho} of Ar), 6.96-7.04 (m, 2H, $\text{N}(\text{C}_6\text{H}_4)\text{S}$, H_{ortho} and meta/N), 6.34-6.39 (m, 1H, $\text{N}(\text{C}_6\text{H}_4)\text{S}$, $\text{H}_{\text{para}}/\text{N}$), 6.15 (s, 1H, $\text{N}(\text{C}_6\text{H}_4)\text{S}$, $\text{H}_{\text{ortho}}/\text{N}$), 1.91 (s, 3H, SCH_3) ppm. $^{13}\text{C}\{^1\text{H}\}$ NMR (CD_2Cl_2 , 75.5 MHz): δ 134.27 (AA'X virtual t, $J_{\text{C,P}}=6.5$ Hz, C-H arom), 134.08 (AA'X virtual t, $J_{\text{C,P}}=1.3$ Hz, C-H arom), 129.87 (AA'X virtual t, $J_{\text{C,P}}=6.2$ Hz, C-H arom), 14.91 (s, SCH_3), C_{quat} not observed. $^{31}\text{P}\{^1\text{H}\}$ NMR (CD_2Cl_2 , 121.5 MHz): δ 34.43 (s) ppm. MS (ESI): m/z 650.00 $[\text{M} - \text{Cl}]^+$, 668.00 $[\text{M} - \text{Cl} + \text{H}_2\text{O}]^+$.

Synthesis of the Nickel(II) Complexes

Synthesis of 12

To a solution of **2** (208 mg, 0.45 mmol) in CH_2Cl_2 (10 mL) was added solid $[\text{NiCl}_2(\text{DME})]$ (99 mg, 0.45 mmol) in one portion. The solution quickly turned orange-red and was stirred at room temperature for 2 h. The solvent was removed under reduced pressure, and the resulting red solid was washed with diethyl ether (2 x 10 mL) and pentane (10 mL). Red crystals suitable for single-crystal X-ray diffraction studies were grown by slow diffusion of pentane into a saturated CH_2Cl_2 solution of **12**. Yield: 260 mg, 98%. Anal. Calcd for $\text{C}_{30}\text{H}_{25}\text{Cl}_2\text{NNiP}_2$ (591.08): C, 60.96; H, 4.26; N, 2.37. Found: C, 60.93; H, 4.21; N, 2.43. FTIR: $\nu_{\max}(\text{solid})/\text{cm}^{-1}$ 3070 w, 3010 w, 2204 w, 1597 m, 1494 m, 1480 m, 1435 m, 1312 w, 1251 s, 1184 w, 1150 w, 1104 s, 1097 s, 1028 w, 995 w, 953 s, 904 s, 763 s, 748 s, 720 m, 688 s, 676 m, 618 w, 561 m, 527 m, 505 s, 480 s, 453 m, 440 m, 409 m. $^1\text{H NMR}$ (CD_2Cl_2 , 300 MHz): δ 8.03 (q, 8H, $^3J_{\text{H,H}}=7.6$ Hz, H_{meta} of Ar), 7.71 (t, 4H, $^3J_{\text{H,H}}=7.6$ Hz, H_{para} of Ar), 7.57 (t, 8H, $^3J_{\text{H,H}}=7.6$ Hz, H_{ortho} of Ar), 6.98-7.05 (m, 3H, $\text{H}_{\text{meta+para}}/\text{N}$), 6.48-6.52 (m, 2H, $\text{H}_{\text{ortho}}/\text{N}$) ppm. $^{31}\text{P}\{^1\text{H}\}$ NMR (CD_2Cl_2 , 121.5 MHz): δ 44.58 (s) ppm. MS (ESI): m/z 490.00 $[\text{M} - \text{NiCl}_4]^{2+}$.

Synthesis of 15

The same procedure was used with **5** (228 mg, 0.45 mmol) and $[\text{NiCl}_2(\text{DME})]$ (99 mg, 0.45 mmol). Red crystals suitable for single-crystal X-ray diffraction studies were grown by slow diffusion of

pentane into a saturated CH_2Cl_2 solution of **15**. Yield: 275 mg, 96%. Anal. Calcd for $\text{C}_{31}\text{H}_{27}\text{Cl}_2\text{NNiP}_2\text{S}$ (637.16): C, 58.44; H, 4.27; N, 2.20. Found: C, 58.60; H, 4.41; N, 2.23. FTIR: $\nu_{\max}(\text{solid})/\text{cm}^{-1}$ 3057 w, 2965 w, 2854 w, 2516 w, 2195 w, 1977 w, 1587 m, 1568 m, 1480 m, 1435 m, 1315 w, 1280 w, 1249 m, 1160 w, 1105 m, 1097 m, 999 m, 989 m, 910 m, 878 w, 834 w, 774 w, 745 s, 719 m, 690 s, 656 m, 576 w, 561 w, 505 s, 495 s, 484 s. $^1\text{H NMR}$ (CD_2Cl_2 , 400 MHz): δ 8.01-8.06 (m, 8H, H_{meta} of Ar), 7.70-7.74 (m, 4H, H_{para} of Ar), 7.56-7.60 (m, 8H, H_{ortho} of Ar), 6.90 (m, 2H, $\text{N}(\text{C}_6\text{H}_4)\text{S}$, H_{ortho} and meta/N), 6.31 (m, 1H, $\text{N}(\text{C}_6\text{H}_4)\text{S}$, $\text{H}_{\text{para}}/\text{N}$), 6.15 (s, 1H, $\text{N}(\text{C}_6\text{H}_4)\text{S}$, $\text{H}_{\text{ortho}}/\text{N}$), 1.93 (s, 3H, SCH_3) ppm. $^{13}\text{C}\{^1\text{H}\}$ NMR (CD_2Cl_2 , 100 MHz): δ 134.01 (AA'X virtual t, $J_{\text{C,P}}=5.6$ Hz, C-H arom), 133.7 (AA'X virtual t, $J_{\text{C,P}}=1.30$ Hz, C-H arom), 129.92 (s, C-H arom), 129.74 (AA'X virtual t, $J_{\text{C,P}}=6.0$ Hz, C-H arom), 127.18 (AA'X virtual t, $J_{\text{C,P}}=25.4$ Hz, C_{ipso} of Ar), 124.35 (s, C-H arom), 120.24 (AA'X virtual t, $J_{\text{C,P}}=3.5$ Hz, C-H arom), 119.77 (AA'X virtual t, $J_{\text{C,P}}=3.0$ Hz, C-H arom), 14.99 (s, SCH_3), 1 C_{quat} not observed. $^{31}\text{P}\{^1\text{H}\}$ NMR (CD_2Cl_2 , 162 MHz): δ 46.35 (s) ppm. MS (ESI): m/z 600.00 $[\text{M} - \text{Cl}]^+$, 618.00 $[\text{M} - \text{Cl} + \text{H}_2\text{O}]^+$.

Complexes **11**, **13** and **14** were synthesized according to the previously published method, obtained in similar yields (86%, 55% and 83% respectively) and their structure and purity confirmed by ^1H , $^{31}\text{P}\{^1\text{H}\}$ and EA analyses.

General Procedures for the Suzuki-Miyaura Catalytic Reactions

$\text{Cs}_2\text{CO}_3/1,4$ -dioxane conditions. Metal complex (x mol%), boronic acid (1.5 mmol), aryl halide (1 mmol), Cs_2CO_3 (2 mmol), hexamethylbenzene or dodecane (0.1 mmol) were placed in a flame-dried 8 mL vial containing a magnetic stirrer. After three vacuum/argon purging cycles, dried and degassed 1,4-dioxane (2 mL) was added under argon and the reaction mixture was heated at 80 °C for 1 h. The reaction was then quenched by rapid cooling and addition of 5 mL of water. The reaction products were extracted with dichloromethane (2 x 10 mL), the combined organic layers were then washed with water (5 mL), brine (5 mL), dried over Na_2SO_4 , and concentrated under reduced pressure. An aliquot of the residue was then used to determine both conversion of starting material and yield of the coupling product by gas chromatography or ^1H NMR analysis with hexamethylbenzene or dodecane as internal standard.

$\text{K}_3\text{PO}_4/\text{tAA}$ conditions. Metal complex (x mol%), boronic acid (1.2 mmol), aryl halide (1 mmol), K_3PO_4 (2 mmol), hexamethylbenzene (0.04 mmol) were placed in a flame-dried 8 mL vial containing a magnetic stirrer. After three vacuum/argon purging cycles, dried and degassed *tert*-amyl alcohol (2 mL) was added under argon and the reaction mixture was heated at 100 °C for 8 h. The reaction was then quenched by rapid cooling and addition of 1 M aqueous HCl (2 mL). The reaction products were extracted with ethyl acetate (2 x 10 mL), the combined organic layers were then washed with water (5 mL), brine (5 mL), dried over Na_2SO_4 , and concentrated under reduced pressure. An aliquot of the residue was then used to determine both conversion of starting material and yield of the coupling product by gas chromatography with hexamethylbenzene as internal standard.

Deposition Number(s) 2314845 (for **6**), 2314846 (for **8.2CHCl₃**), 2314847 (for **12**) and 2314848 (for **15**) contain(s) the supplementary crystallographic data for this paper. These data are provided free of charge by the joint Cambridge Crystallographic Data Centre and Fachinformationszentrum Karlsruhe Access Structures service.

Author Contributions

VF; investigation, formal analysis, writing research reports. DDS; investigation, formal analysis, writing research reports. JCD; investigation (X-ray diffraction). SL–M; investigation (X-ray diffraction). PG; conceptualization, funding acquisition, supervision, writing – review and editing. CF; conceptualization, supervision, writing – review and editing.

Acknowledgements

We gratefully acknowledge funding by the ANR (Agence Nationale de la Recherche) through the NiCatEther project (grant ANR-22-CE07-0029-01) and by the CNRS (Centre National de la Recherche Scientifique). We thank Sandric Afonso, Billal Karouach and Laurent Caville for performing some catalytic reactions and GC analyses.

Conflict of Interests

The authors declare no conflict of interest.

Data Availability Statement

Accessible, Interoperable and Reusable (FAIR) data related to this publication will be deposited in the HAL repository (<https://hal.science>) under the DOI of the present publication.

Keywords: Palladium · Nickel · Phosphine · Catalysis · Suzuki-Miyaura Cross-coupling · Small bite angle ligand · green reaction conditions.

- [1] P. C. J. Kamer, P. W. N. M. van Leeuwen, Phosphorus(III) Ligands in Homogeneous Catalysis: Design and Synthesis, Wiley, New-York, 2012.
- [2] P. W. N. M. van Leeuwen, P. C. J. Kamer, J. N. H. Reek, P. Dierkes, *Chem. Rev.* 2000, 100, 2741–2770.
- [3] P. von Matt, A. Pfaltz, *Angew. Chem. Int. Ed.* 1993, 32, 566–568.
- [4] H. A. McManus, P. J. Guiry, *Chem. Rev.* 2004, 104, 4151–4202.
- [5] D. Pugh, A. A. Danopoulos, *Coord. Chem. Rev.* 2007, 251, 610–641.
- [6] H. Salem, M. Schmitt, U. Herrlich, E. Kühnel, M. Brill, P. Nägele, A. L. Bogado, F. Rominger, P. Hofmann, *Organometallics* 2013, 32, 29–46.
- [7] C. Fliedel, A. Labande, E. Manoury, R. Poli, *Coord. Chem. Rev.* 2019, 394, 65–103.
- [8] M.-N. Birkholz, Z. Freixa, P. W. N. M. van Leeuwen, *Chem. Soc. Rev.* 2009, 38, 1099–1118.
- [9] H. Clavier, S. P. Nolan, *Chem. Commun.* 2010, 46, 841–861.
- [10] J. De Tovar, F. Rataboul, L. Djakovitch, *ChemCatChem* 2020, 12, 5797–5808.
- [11] R. J. Puddephatt, *Chem. Soc. Rev.* 1983, 12, 99–127.
- [12] M. S. Balakrishna, V. S. Reddy, S. S. Krishnamurthy, J. F. Nixon, J. C. T. R. Burkett St. Laurent, *Coord. Chem. Rev.* 1994, 129, 1–90.
- [13] M. Witt, H. W. Roesky, *Chem. Rev.* 1994, 94, 1163–1181.
- [14] P. Bhattacharyya, J. D. Woollins, *Polyhedron* 1995, 14, 3367–3388.
- [15] T. Appleby, J. D. Woollins, *Coord. Chem. Rev.* 2002, 235, 121–140.
- [16] C. Fliedel, A. Ghisolfi, P. Braunstein, *Chem. Rev.* 2016, 116, 9237–9304.
- [17] S. M. Mansell, *Dalton Trans.* 2017, 46, 15157–15174.
- [18] C. Fliedel, R. Pattacini, P. Braunstein, *J. Cluster Sci.* 2010, 21, 397–415.
- [19] V. Rosa, C. Fliedel, A. Ghisolfi, R. Pattacini, T. Aviles, P. Braunstein, *Dalton Trans.* 2013, 42, 12109–12119.
- [20] C. Fliedel, V. Rosa, A. Falceto, P. Rosa, S. Alvarez, P. Braunstein, *Inorg. Chem.* 2015, 54, 6547–6559.
- [21] C. Fliedel, V. Rosa, B. Vileno, N. Parizel, S. Choua, C. Gourlaouen, P. Rosa, P. Turek, P. Braunstein, *Inorg. Chem.* 2016, 55, 4183–4198.
- [22] A. Ghisolfi, C. Fliedel, P. de Frémont, P. Braunstein, *Dalton Trans.* 2017, 46, 5571–5586.
- [23] C. Fliedel, V. Faramarzi, V. Rosa, B. Doudin, P. Braunstein, *Chem. Eur. J.* 2014, 20, 1263–1266.
- [24] A. Ghisolfi, C. Fliedel, V. Rosa, K. Y. Monakhov, P. Braunstein, *Organometallics* 2014, 33, 2523–2534.
- [25] C. Fliedel, R. Poli, *Coord. Chem. Rev.* 2018, 355, 1–26.
- [26] A. Ghisolfi, C. Fliedel, V. Rosa, R. Pattacini, A. Thibon, K. Y. Monakhov, P. Braunstein, *Chem. Asian J.* 2013, 8, 1795–1805.
- [27] M. Chen, C. Chen, *Angew. Chem. Int. Ed.* 2018, 57, 3094–3098.
- [28] K. A. Alferov, G. P. Belov, Y. Meng, *Appl. Catal. A* 2017, 542, 71–124.
- [29] D. S. McGuinness, *Chem. Rev.* 2011, 111, 2321–2341.
- [30] T. Agapie, *Coord. Chem. Rev.* 2011, 255, 861–880.
- [31] C. C. C. Johansson Seechurn, M. O. Kitching, T. J. Colacot, V. Snieckus, *Angew. Chem. Int. Ed.* 2012, 51, 5062–5085.
- [32] D. Wang, D. Astruc, *Chem. Rev.* 2015, 115, 6621–6686.
- [33] K. P. Bryliakov, A. A. Antonov, *J. Organomet. Chem.* 2018, 867, 55–61.
- [34] P. Devendar, R.-Y. Qu, W.-M. Kang, B. He, G.-F. Yang, *J. Agric. Food Chem.* 2018, 66, 8914–8934.
- [35] K. W. Anderson, S. L. Buchwald, *Angew. Chem. Int. Ed.* 2005, 44, 6173–6177.
- [36] J. Yang, S. Liu, J.-F. Zheng, J. Zhou, *Eur. J. Org. Chem.* 2012, 2012, 6248–6259.
- [37] E. B. Landstrom, S. Handa, D. H. Aue, F. Gallou, B. H. Lipshutz, *Green Chem.* 2018, 20, 3436–3443.
- [38] B. S. Takale, R. R. Thakore, S. Handa, F. Gallou, J. Reilly, B. H. Lipshutz, *Chem. Sci.* 2019, 10, 8825–8831.
- [39] T. Mesganaw, N. K. Garg, *Org. Process Res. Dev.* 2013, 17, 29–39.
- [40] S. D. Ramgren, L. Hie, Y. Ye, N. K. Garg, *Org. Lett.* 2013, 15, 3950–3953.
- [41] L. Hie, N. F. Fine Nathel, T. K. Shah, E. L. Baker, X. Hong, Y.-F. Yang, P. Liu, K. N. Houk, N. K. Garg, *Nature* 2015, 524, 79–83.
- [42] N. A. Weires, E. L. Baker, N. K. Garg, *Nat. Chem.* 2016, 8, 75–79.
- [43] U. Beckmann, D. Süslüyan, P. C. Kunz, *Phosphorus, Sulfur, Silicon Relat. Elem.* 2011, 186, 2061–2070.
- [44] D. W. Allen, B. F. Taylor, *J. Chem. Soc. Dalton Trans.* 1982, 51–54.
- [45] H. A. Bent, *Chem. Rev.* 1961, 61, 275–311.
- [46] M. L. Kelty, A. J. McNeece, J. W. Kurutz, A. S. Filatov, J. S. Anderson, *Chem. Sci.* 2022, 13, 4377–4387.
- [47] K. G. Gaw, M. B. Smith, A. M. Z. Slawin, *New J. Chem.* 2000, 24, 429–435.
- [48] F. Durap, N. Biricik, B. Gümgüm, S. Özkar, W. H. Ang, Z. Fei, R. Scopelliti, *Polyhedron* 2008, 27, 196–202.
- [49] N. Biricik, C. Kayan, B. Gümgüm, Z. Fei, R. Scopelliti, P. J. Dyson, N. Gürbüz, İ. Özdemir, *Inorg. Chim. Acta* 2010, 363, 1039–1047.
- [50] L. Yang, D. R. Powell, R. P. Houser, *Dalton Trans.* 2007, 955–964.
- [51] A. Okuniewski, D. Rosiak, J. Chojnacki, B. Becker, *Polyhedron* 2015, 90, 47–57.
- [52] Z. Sun, F. Zhu, Q. Wu, S.-a. Lin, *Appl. Organomet. Chem.* 2006, 20, 175–180.
- [53] W. Seidel, M. Alexiev, *Z. Anorg. Allg. Chem.* 1978, 438, 68–74.
- [54] D. Kistamurthy, S. Otto, J. Moss, G. Smith, *Transition Met. Chem.* 2010, 35, 633–637.
- [55] Z. Weng, S. Teo, T. S. A. Hor, *Dalton Trans.* 2007, 2007, 3493–3498.
- [56] A. Bollmann, K. Blann, J. T. Dixon, F. M. Hess, E. Killian, H. Maumela, D. S. McGuinness, D. H. Morgan, A. Neveling, S. Otto, M. Overett, A. M. Z. Slawin, P. Wasserscheid, S. Kuhlmann, *J. Am. Chem. Soc.* 2004, 126, 14712–14713.
- [57] E. Killian, K. Blann, A. Bollmann, J. T. Dixon, S. Kuhlmann, M. C. Maumela, H. Maumela, D. H. Morgan, P. Nongodlwana, M. J. Overett, M. Pretorius, K. Höfener, P. Wasserscheid, *J. Mol. Catal. A* 2007, 270, 214–218.
- [58] I. M. Aladzheva, O. V. Bykhovskaya, A. A. Vasil'ev, Y. V. Nelyubina, Z. S. Klemenkova, *Russ. Chem. Bull., Int. Ed.* 2015, 64, 909–913.
- [59] M. Aydemir, A. Baysal, B. Gümgüm, *J. Organomet. Chem.* 2008, 693, 3810–3814.
- [60] N. Biricik, F. Durap, C. Kayan, B. Gümgüm, N. Gürbüz, İ. Özdemir, W. H. Ang, Z. Fei, R. Scopelliti, *J. Organomet. Chem.* 2008, 693, 2693–2699.
- [61] O. Akba, F. Durap, M. Aydemir, A. Baysal, B. Gümgüm, S. Özkar, *J. Organomet. Chem.* 2009, 694, 731–736.
- [62] M. Aydemir, A. Baysal, E. Sahin, B. Gümgüm, S. Ozkar, *Inorg. Chim. Acta* 2011, 378, 10–18.
- [63] C. Kayan, N. Biricik, M. Aydemir, *Transition Met. Chem.* 2011, 36, 513–520.

- [64] C. Kayan, N. Biricik, M. Aydemir, R. Scopelliti, *Inorg. Chim. Acta* **2012**, *385*, 164–169.
- [65] P.-C. Ioannou, C. Arbez-Gindre, M. Zoumpantioti, C. P. Raptopoulou, V. Psycharis, I. D. Kostas, P. Kyritsis, *J. Organomet. Chem.* **2019**, *879*, 40–46.
- [66] W. L. Steffen, G. J. Palenik, *Inorg. Chem.* **1976**, *15*, 2432–2439.
- [67] M.-Q. Yan, J. Yuan, F. Lan, S.-H. Zeng, M.-Y. Gao, S.-H. Liu, J. Chen, G.-A. Yu, *Org. Biomol. Chem.* **2017**, *15*, 3924–3929.
- [68] D. Wang, H.-G. Chen, X.-C. Tian, X.-X. Liang, F.-Z. Chen, F. Gao, *RSC Adv.* **2015**, *5*, 107119–107122.
- [69] F.-S. Han, *Chem. Soc. Rev.* **2013**, *42*, 5270.
- [70] L. Falivene, Z. Cao, A. Petta, L. Serra, A. Poater, R. Oliva, V. Scarano, L. Cavallo, *Nat. Chem.* **2019**, *11*, 872–879.
- [71] L. Falivene, R. Credendino, A. Poater, A. Petta, L. Serra, R. Oliva, V. Scarano, L. Cavallo, *Organometallics* **2016**, *35*, 2286–2293.
- [72] B. M. Rosen, K. W. Quasdorf, D. A. Wilson, N. Zhang, A.-M. Resmerita, N. K. Garg, V. Percec, *Chem. Rev.* **2011**, *111*, 1346–1416.
- [73] B. S. Kadu, *Catal. Sci. Technol.* **2021**, *11*, 1186–1221.
- [74] B. A. Baviskar, P. V. Ajmire, D. S. Chumbhale, M. S. Khan, V. G. Kuchake, M. Singupuram, P. R. Laddha, *Sustain. Chem. Pharm.* **2023**, *32*, 100953.
- [75] I. Stamatopoulos, M. Plaček, V. Psycharis, A. Terzis, J. Svoboda, P. Kyritsis, J. Vohlidal, *Inorg. Chim. Acta* **2012**, *387*, 390–395.
- [76] I. Stamatopoulos, D. Giannitsios, V. Psycharis, C. P. Raptopoulou, H. Balcar, A. Zukal, J. Svoboda, P. Kyritsis, J. Vohlidal, *Eur. J. Inorg. Chem.* **2015**, *2015*, 3038–3044.
- [77] P.-C. Ioannou, R. Coufal, K. Kakridi, C. P. Raptopoulou, O. Trhlíková, V. Psycharis, J. Zedník, P. Kyritsis, J. Vohlidal, *RSC Adv.* **2022**, *12*, 2227–2236.
- [78] C. Ercolani, J. V. Quagliano, L. M. Vallarino, *Inorg. Chim. Acta* **1973**, *7*, 413–422.
- [79] Y.-L. Zhao, Y. Li, S.-M. Li, Y.-G. Zhou, F.-Y. Sun, L.-X. Gao, F.-S. Han, *Adv. Synth. Catal.* **2011**, *353*, 1543–1550.
- [80] Ł. Banach, J. Robaszkiewicz, P. Pawluć, *J. Catal.* **2024**, *436*, 115635.
- [81] J. E. Borowski, S. H. Newman-Stonebraker, A. G. Doyle, *ACS Catal.* **2023**, *13*, 7966–7977.
- [82] B.-T. Guan, Y. Wang, B.-J. Li, D.-G. Yu, Z.-J. Shi, *J. Am. Chem. Soc.* **2008**, *130*, 14468–14470.
- [83] A. Boudier, P.-A. R. Breuil, L. Magna, H. Olivier-Bourbigou, P. Braunstein, *J. Organomet. Chem.* **2012**, *718*, 31–37.
- [84] G. M. Sheldrick, *Acta Crystallogr. Sect. A* **2015**, *A71*, 3–8.
- [85] G. M. Sheldrick, *Acta Crystallogr. Sect. C* **2015**, *C71*, 3–8.
- [86] J. Farrugia, *J. Appl. Crystallogr.* **1997**, *30*, 565–565.
- [87] M. N. Burnett, C. K. Johnson, Report ORNL-6895. Oak Ridge National Laboratory, Tennessee, USA **1996**.

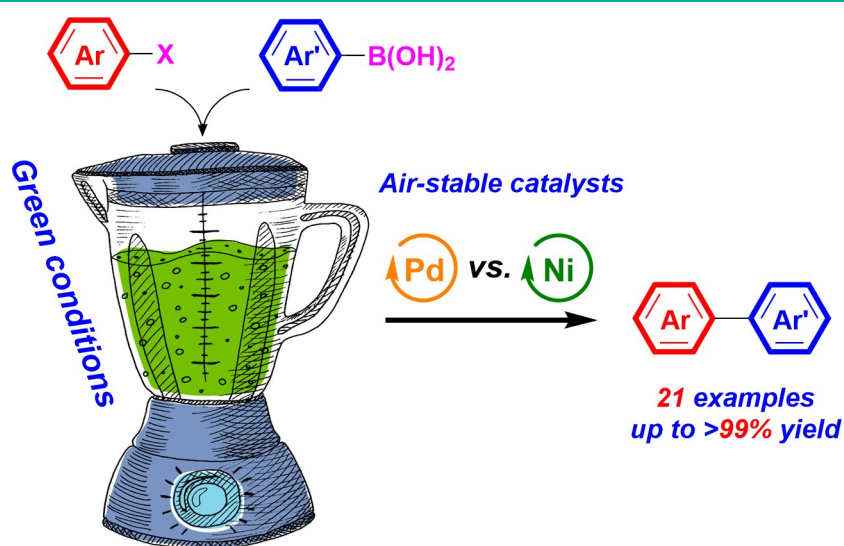
Manuscript received: November 1, 2024

Revised manuscript received: December 13, 2024

Accepted manuscript online: January 7, 2025

Version of record online: ■■, ■■

RESEARCH ARTICLE



V. Fagué, D. Dos Santos, J.-C. Daran, S. Mallet-Ladeira, P. Guillo*, C. Fliedel*

1 – 17

(*P,N,P*)Pd- versus (*P,N,P*)Ni-Catalyzed Suzuki-Miyaura Cross-Coupling Reactions under Green Conditions[†]

Which one performs at the best? A comparative study between palladium and nickel complexes of *N*-substituted/functionalized bis-

(diphenylphosphino)amine-type ligands applied to Suzuki-Miyaura cross-coupling reactions under green conditions.